

1 **Experimental Models of Short Courses of Liposomal Amphotericin B for**
2 **Induction Therapy for Cryptococcal Meningitis**

3

4 Jodi Lestner,^{a,#} Laura McEntee,^a Adam Johnson,^a Joanne Livermore,^a Sarah Whalley,^a

5 Julie Schwartz,^b John R. Perfect,^c Thomas Harrison,^d William Hope^a

6

7 Antimicrobial Pharmacodynamics and Therapeutics, Department of Molecular and

8 Clinical Pharmacology, University of Liverpool, Liverpool, UK^a; Charles River

9 Laboratories, Davis, CA, USA^b; Department of Medicine, Duke University, Durham,

10 North Carolina, USA^c; Research Centre for Infection and Immunity, St George's

11 University of London, London, UK^d

12

13 Running Title: Abbreviated induction for cryptococcal meningitis

14

15 Address correspondence to

16 Jodi Lestner, University of Liverpool, Sherrington Building, Ashton Street, Liverpool

17 L69 3GE, United Kingdom

18 Tel: +44 (0)151 794 5941

19 Email: jlestner@liverpool.ac.uk

20

21

22

23

24

25 **ABSTRACT**

26 Cryptococcal meningoencephalitis is a rapidly lethal infection in
27 immunocompromised patients. Induction regimens are usually administered for 2-
28 weeks. The shortest effective period of induction therapy with liposomal
29 amphotericin B (LAmB) is unknown. The pharmacodynamics of LAmB were studied
30 in murine and rabbit models of cryptococcal meningoencephalitis. The
31 concentrations of LAmB in plasma and brain of mice were measured using HPLC.
32 Histopathological changes were determined. The penetration of LAmB into the brain
33 was determined by immunohistochemistry using an antibody directed to amphotericin
34 B. A dose-dependent decline in fungal burden was observed in the brain of mice with
35 near-maximal efficacy achieved with LAmB 10-20 mg/kg/day. The terminal
36 elimination half-life in brain was 133 hours. The pharmacodynamics of a single dose
37 of 20 mg/kg was the same as 20 mg/kg/day administered for 2 weeks. Changes in
38 quantitative counts were reflected by histopathological changes in the brain. Three
39 doses of LAmB 5 mg/kg/day in rabbits were required to achieve fungicidal activity in
40 cerebrospinal fluid (cumulative AUC 2500 mg.h/L). Amphotericin B was visible in
41 the intra- and perivascular spaces, leptomeninges and choroid plexus. The prolonged
42 mean residence time of amphotericin B in the brain suggest abbreviated induction
43 regimens of LAmB are possible for cryptococcal meningoencephalitis.

44

45 Key words. Liposomal amphotericin B, pharmacokinetics, pharmacodynamics,
46 *Cryptococcus neoformans*, cryptococcal meningitis, meningoencephalitis

47

48

49

50 **INTRODUCTION**

51 Cryptococcal meningitis is a common and frequently lethal disease in patients with
52 HIV/AIDS (1). Rapid fungicidal activity in cerebrospinal fluid (CSF) is associated
53 with better clinical outcomes and improved survival (2). Amphotericin B
54 deoxycholate (DAmB) is the most potent amphotericin B formulation on a mg-mg
55 basis (3, 4). While effective, DAmB is toxic and associated with significant infusion-
56 related toxicity, nephrotoxicity and anemia (5, 6). Furthermore, DAmB is not orally
57 bioavailable, and must be injected. The need for rapid reliable monitoring for side
58 effects and for intravenous administration means that amphotericin B-based treatment
59 is simply not possible in many resource-poor settings. Hence, the best current therapy
60 cannot be administered to patients in many countries where the prevalence of
61 cryptococcal meningitis is the highest. In these cases, the only alternative agent is
62 fluconazole, but even with the use of high doses (800-1200 mg/day), fungicidal
63 activity in CSF and clinical outcomes are suboptimal (7, 8). Alternative approaches
64 are urgently required.

65
66 There is surprisingly little evidence for the use of liposomal amphotericin B (LAmB)
67 for cryptococcal meningitis. Preclinical and clinical data suggest 3-6 mg/kg/day is a
68 safe and effective regimen (9, 10). Typically, the duration of amphotericin B-based
69 induction regimens is 2 weeks, primarily based on surrogate mycological markers of
70 early fungicidal activity such as CSF sterilization (11, 12). The shortest duration of
71 LAmB that is maximally effective is not known. We recently demonstrated that an
72 abbreviated course of DAmB (3 days) may be as effective as 2 weeks of therapy (13)
73 and short courses of DAmB (in combination with fluconazole) are associated with
74 rapid clearance of the CSF in patients with cryptococcal meningitis (14). Thus, there

75 is a precedent and rationale for examining the safety and efficacy of abbreviated
76 regimens of LAmB as induction therapy for cryptococcal meningitis.

77

78 Here, we used two previously described (15, 16) and well-characterised laboratory
79 animal models of cryptococcal meningitis to study the pharmacodynamics of
80 abbreviated courses of liposomal amphotericin B. Our principal goal was to provide
81 the experimental evidence underpinning Phase II and III clinical trials examining the
82 efficacy of abbreviated regimens of LAmB.

83

84 **METHODS**

85 **Strain and In vitro Susceptibility Testing**

86 *Cryptococcus neoformans* var. *grubii* (ATCC 208821 or H99) was the challenge organism for
87 experiments in mice and rabbits. The minimum inhibitory concentration (MIC)
88 testing was performed using European Committee on Antimicrobial Susceptibility
89 Testing (EUCAST) and Clinical Laboratory Sciences Institute (CLSI) methodology.
90 MICs were determined in three independently conducted experiments.

91

92 **Laboratory Animal Models of Cryptococcal meningoencephalitis.**

93 All murine studies were performed under UK Home Office project licence PPL
94 40/3630 and received prior approved by the ethics committee at the University of
95 Liverpool. Two models of cryptococcal meningitis were used that provide
96 complementary information on the time course of cryptococcal meningoencephalitis,
97 and the response to treatment with LAmB. The murine model has the advantage of
98 being highly reproducible. In this model, the fungal burden in the cerebrum is the
99 primary read-out and quantitative counts in the CSF cannot be obtained. In contrast,

100 the rabbit model enables the time course of fungal burden in the CSF to be
101 determined, which is a clinically relevant sub-compartment within the central nervous
102 system. The fungal burden in other central nervous system sub-compartments is also
103 available (e.g. cerebrum, vitreous, meninges), but only at the time of sacrifice.

104

105 For the murine model, immunosuppression is not required because mice are
106 inherently susceptible to disseminated cryptococcal infection. An inoculum of 3×10^8
107 CFU in 0.25 mL PBS was injected i.v. via the lateral tail vein, which results in a
108 highly reproducible encephalitis. Mortality occurs at the latter part of the second
109 week of infection meaning that early death does not confound any assessment of
110 fungal burden in the initial 7-10 days of infection. The intended inoculum was
111 confirmed using quantitative counts after each experiment. The limit of detection for
112 quantitative culture was $1.2 \log_{10}$ CFU/g.

113

114 A rabbit model of cryptococcal meningoencephalitis that was originally developed
115 and described by Perfect et al. (15) was used to study the impact of abbreviated
116 regimens on the time course of fungal burden in the CSF. Briefly, *C. neoformans*
117 inocula were grown in Yeast Extract-Peptone-Dextrose (YPD) broth to a final
118 concentration of $3 \pm 0.25 \times 10^8$ CFU/mL. Inoculum concentrations were estimated by
119 optical density and confirmed by quantitative culture. Anaesthetized rabbits were
120 infected via cisternal injection with an inoculum volume of 0.3 mL. Rabbits were
121 anesthetized at day +2, 5, 7 and 11 post-inoculation. CSF was obtained via cisternal
122 puncture. A 1 mL sample was removed at each time point. All rabbits were sacrificed
123 at the end of the experiment, which was 13 days post inoculation. A final CSF
124 sample was obtained immediately after sacrifice. In addition, the fungal burden in the

125 cerebrum at the end of the study period was determined as an additional endpoint.
126 Representative samples of cerebrum were homogenized in 2 mL of Phosphate-
127 Buffered Saline (PBS). Homogenate and CSF were then plated to Sabouraud
128 Dextrose Agar (SDA) containing chloramphenicol.

129

130 **Pharmacokinetic and Pharmacodynamic (PK-PD) Studies**

131 The PK-PD relationships in mice were determined over the course of multiple
132 independently conducted experiments. The time-course of infection in the cerebrum
133 was determined using a destructive design in which groups of CD-1 mice (n=3 per
134 group) were sacrificed at predefined intervals between 0 and 240 hours post
135 inoculation. Treatment was commenced 24-hours post inoculation. Dose finding
136 studies were conducted using 0.5-20 mg/kg/day. Each experiment incorporated an
137 untreated control and at least two experimental arms (n=15 per arm). Each dosing
138 regimen was repeated in triplicate. Data from subjects requiring sacrifice on humane
139 grounds were included in analyses at the time of death.

140

141 The PK in plasma and cerebrum were determined in a separate experiment and once
142 the relevant dose-response relationships had been determined. The PK was
143 determined in infected mice. PK data were obtained at two intervals (immediately
144 following the initiation of therapy and then after 5 days of dosing). Groups of mice
145 (n=3) were sacrificed 0.5, 1, 2, 6 and 24 hours post drug administration. Plasma was
146 obtained by terminal cardiac puncture, placed immediately on ice, centrifuged and
147 stored at -80°C for analysis. The cerebrum was extracted at the time of necropsy
148 under sterile conditions. One hemisphere was submitted for quantitative cultures
149 while the other was stored for future measurement of amphotericin B concentrations.

150

151 PK-PD relationships were studied following various induction regimens, as follows.

152 A single dose of 5 mg/kg was studied based on previous studies in invasive
153 pulmonary aspergillosis. Groups of rabbits received a single dose, 3 doses of 5
154 mg/kg/day and daily therapy of 5 mg/kg/day.

155

156 **Measurement of amphotericin B concentrations**

157 The concentrations of amphotericin B were estimated using a previously described
158 assay (3). The limit of detection was 0.05 mg/L. The intra and inter-day variation
159 was <7%.

160

161 **Histopathology and staining of LAmB in the central nervous system of mice**

162 The brain was collected and placed into 10% neutral buffered formalin for
163 histopathologic evaluation. Formalin fixed tissues were trimmed, cryoprotected by
164 sucrose replacement, then embedded in OCT freezing media. Approximately 5 μ m
165 sections were prepared for staining.

166

167 A commercially available mouse monoclonal antibody directed against *Cryptococcus*
168 *neoformans* was used to determine the extent of infection (MyBioSource, LLC, San
169 Diego, CA). Yeasts stained consistently and intensely (4+) positive with the anti-C.
170 neoformans antibody. The yeasts did not stain with the species-, isotype-, and
171 concentration- matched negative control antibody (mouse IgG1 (Ms IgG1)) that was
172 substituted for the Ms anti-C. neoformans reagent (data not shown).

173

174 Amphotericin B was visualised using an affinity-purified rabbit anti-amphotericin B
 175 antibody (Antibodies Inc., Davis, CA). Immunohistochemistry was performed using
 176 standard immunoperoxidase and alkaline phosphatase methodology, and validated by
 177 appropriate and reproducible positive and negative controls for staining amphotericin
 178 B as previously described (17, 18).

179

180 **Mathematical Modelling**

181 The murine PK and PD data from mice were modelled using a population
 182 methodology with the program Pmetrics (19). The mean drug concentration, cerebral
 183 concentration and fungal burden in the cerebrum from groups of 3 mice were used.
 184 All data were weighted by the observed variance from each group of mice for drug
 185 concentrations and fungal burden. The structural model took the form:

186

$$\frac{dX(1)}{dt} = R(1) - \left(\frac{SCL}{Vc} + K_{cp} + K_{cb} \right) \times X(1) + K_{bc} \times X(3) + K_{pc} \times X(2)$$

$$\frac{dX(2)}{dt} = -K_{pc} \times X(2) + K_{cp} \times X(1)$$

$$\frac{dX(3)}{dt} = K_{cb} \times X(1) - K_{bc} \times X(3)$$

$$\frac{dN}{dt} = K_g \max \times \left(1 - \left(\frac{\frac{X(3)^{Hg}}{V_m}}{\frac{X(3)^{Hg}}{V_m} + C_{50g}^{Hg}} \right) \right) \times \left(1 - \frac{N}{POP_{MAX}} \right) \times N$$

187

188 Where X(1), X(2) and X(3) represent the amount of amphotericin B (mg) in the
 189 central compartment, peripheral compartment and cerebrum, respectively. N is the
 190 number of organisms in the cerebrum. R(1) represents the i.v. injection of liposomal
 191 amphotericin B (mg); K_{cb}, K_{bc}, K_{cp} and K_{pc} represent the first-order rate constants

192 connecting the various compartments. H_g is the slope function for the suppression of
 193 growth. K_{gmax} is the maximum rate of fungal growth in the brain; V_m is the volume
 194 of the murine brain; C_{50g} is the concentration of amphotericin B in the brain at which
 195 there is half-maximal inhibition of growth, and POP_{MAX} is the maximum theoretical
 196 density of organisms in the brain.

197

198 Equation 1 describes the movement of liposomal amphotericin B into and out of the
 199 central compartment (plasma). Equation 2 describes the movement of liposomal
 200 amphotericin B into and out of the peripheral compartment. Equation 3 describes the
 201 movement of drug into the brain. Equation 4 describes the pharmacodynamics of
 202 amphotericin B. This equation contains terms that describe the capacity-limited
 203 fungal growth in the brain, and drug induced suppression of the fungal growth.

204 The fit of the mathematical model to the combined PK and PD dataset from mice was
 205 assessed using the log likelihood value, measures of precision and bias and visual
 206 inspection of the observed-versus-predicted values both before and after the Bayesian
 207 step, and assessment of the linear regression of the observed-versus-predicted values
 208 both before and after the Bayesian step. Inspection of the PK of liposomal
 209 amphotericin B in rabbits suggested that the volume of distribution contracted with
 210 time, as recently described by us in children (20).

211

$$\frac{dX(1)}{dt} = R(1) - \left(\frac{SCL}{X(3)} + K_{cp} \right) \times X(1) + K_{pc} \times X(2)$$

$$\frac{dX(2)}{dt} = K_{cp} \times X(1) - K_{pc} \times X(2)$$

$$\frac{dX(3)}{dt} = -X(3) * K + V_{fin}$$

212 with output equation

$$Y(1) = \frac{X(1)}{X(3)}$$

213 Where X(1) and X(2) is the amount of liposomal amphotericin B in the central and
214 peripheral compartment, respectively. SCL is the clearance of drug from the central
215 compartment, and Kcp and Kpc are the two first order inter-compartmental rate
216 constants connecting the central and peripheral compartments. X(3) is the volume of
217 the central compartment that contracts with time according to equation 3. X(3) has an
218 initial volume, Vini, which is estimated as an initial condition in Pmetrics. The
219 volume contracts over time according to the first order rate constant K. The final
220 volume after prolonged drug administration is Vfin. Equation 1 describes the rate of
221 change of the amount of liposomal amphotericin B in the central compartment.
222 Equation 2 describes the rate of change of the amount of liposomal amphotericin B in
223 the peripheral compartment.

224

225 **PK-PD Bridging Studies**

226 In order to place the experimental findings in a clinical context we bridged the
227 preclinical PK-PD findings from mice and rabbits to patients using a previously
228 described population PK model for liposomal amphotericin B (21). This model was
229 used to estimate the average drug exposure (quantified in terms of AUC) resulting
230 from various human doses.

231

232 **RESULTS**

233 **Dose-Exposure-Response Relationships in Mice**

234 Liposomal amphotericin B was well tolerated in mice with no observed toxicity
235 following rapid intravenous (i.v.) injection. There was a clear dose-response
236 relationship with doses of 0.5-20 mg/kg/day. Fungicidal activity was not observed

237 (i.e. we did not observe a decline in \log_{10} CFU/g following daily therapy). Rather, a
238 fungistatic effect was seen whereby the infection at the time of drug administration 24
239 hours post inoculation was stabilised. Near maximal antifungal activity was observed
240 following treatment with 10-20 mg/kg/day and with an AUC:MIC of approximately
241 100 (Figure 1).

242

243 A profound and durable antifungal effect was apparent following a single dose of 20
244 mg/kg in mice (Figure 3). There was no evidence of significant fungal regrowth after
245 240 hours of observation. The persistent antifungal effect may be explained by the
246 long terminal half-life of amphotericin B in the plasma and cerebrum (circa. 113
247 hours; Figure 2).

248

249 **Histopathology and Immunohistochemistry in Mice**

250 The persistent antifungal effect evident from the \log_{10} CFU/g data was mirrored by
251 histopathological findings shown in Figure 3. In mice receiving vehicle only,
252 cryptococcal meningoencephalitis manifested as a multifocal disease with cyst-like
253 cavities filled with multiple encapsulated organisms approximately 6-10 μ m in
254 diameter. There was no evidence of an inflammatory component within or around the
255 cavities.

256

257 Mouse liver (harvested from mice receiving a total cumulative liposomal
258 amphotericin B dose of 225 mg/kg) was used as positive control tissue in all
259 amphotericin B localization experiments. Moderate to marked staining of frequent
260 Kupffer cells was observed in the positive control tissue. All other tissue elements
261 were negative. There was no staining of Kupffer cells when a species-, isotype-, and

262 concentration-matched negative control antibody (rabbit IgG) was substituted for the
263 rabbit anti-AMB reagent. Kupffer cells in control mouse liver that received 5%
264 dextrose did not stain with rabbit anti-AMB reagent.

265

266 There was differential penetration of amphotericin B into the brain (Figure 5).
267 Staining was apparent early (i.e. one-hour post dose) and in both intravascular and
268 perivascular spaces, suggesting the drug crossed the blood-brain-barrier. Staining
269 was especially prominent in blood vessels in the leptomeninges and choroid plexus, as
270 well as small cerebral capillaries. Staining was both extra- and intra-cellular.
271 Granular extracellular staining was observed in and surrounding blood vessels.
272 Intracellular cytoplasmic staining was observed in mononuclear/microglial cells.
273 Positive circulating mononuclear cells (presumptive monocytes) were identified in
274 cerebral capillaries. Additional extracellular staining was observed in the ventricular
275 system associated with the ependymal lining suggesting entry into the cerebral spinal
276 fluid. In contrast, staining was not observed in the normal cerebral tissue or in
277 residual cryptococcomas after 10 days of treatment with LAmB at doses 10 or 20
278 mg/kg/day.

279

280 **Mathematical Pharmacokinetic-Pharmacodynamic Model in Mice**

281 The fit of the mathematical model to the combined murine PK-PD dataset was
282 acceptable, even though fitting was difficult. The estimates for the parameters are
283 summarized in Table 1. The principal challenge was modelling the depot-like effect
284 of LAmB in the brains of mice where low drug concentrations were observed to have
285 exerted an antifungal effect that lasted well beyond the time that liposomal
286 amphotericin B concentrations were detectable.

287

288 **Pharmacokinetic-Pharmacodynamic Relationships in Rabbits**

289 The mean parameter values best accounted for the observed PK data. The parameter
290 values were as follows: SCL 0.018 ± 0.008 L/h; Kcp 10.37 ± 0.416 h⁻¹; Kpc $26.09 \pm$
291 0.96 h⁻¹; K 0.093 ± 0.04 h⁻¹; Vini 4.717 ± 0.233 L and Vfin 0.003 ± 0.002 L. The
292 coefficient of determination for the linear regression before and after the Bayesian
293 step was 0.87 and 0.98, respectively and in both cases the intercept and slope
294 approximated zero and one, respectively.

295

296 The pharmacodynamics in rabbits similarly illustrated the potential utility of
297 abbreviated LAmB induction but differed somewhat to those observed in mice. A
298 single dose of LAmB at 5 mg/kg appeared fungistatic only up to 264 hours, and did
299 not provide a durable response in CSF or cerebrum ($\Delta \log_{10}$ CFU/g = 1.9 ± 1.2 and
300 $\Delta \log_{10}$ CFU/g = 3.2 ± 0.5 , respectively), despite higher estimated AUC₀₋₂₄ compared
301 to mice receiving a single dose of 20 mg/kg (820 ± 15 vs. 580 ± 30 mg.h/L). Three
302 doses of LAmB at 5 mg/kg administered every 24 hours (and commencing 48 hours
303 post inoculation) induced a prompt decline in fungal burden in the CSF and cerebrum
304 ($\Delta \log_{10}$ CFU/mL = -2.8 ± 0.8 and $\Delta \log_{10}$ CFU/g = -0.1 ± 0.4 , respectively). This
305 regimen produced a cumulative total AUC₄₈₋₁₂₀ of 2,499 mg.h/L. The effect of this
306 abbreviated regimen in rabbits was comparable to that achieved with daily therapy
307 (Figure 6).

308

309 The exposure-response relationships in the cerebrum of rabbits were similar. The
310 fungal density (\log_{10} CFU/g mean \pm standard deviation) for controls, 5 mg/kg once, 5
311 mg/kg/day for three days and 5 mg/kg/day was 5.92 ± 0.55 , 5.21 ± 1.20 , 2.43 ± 1.23

312 and 2.47 ± 0.70 , respectively. Thus, in comparison to the murine studies, > 1 day of
313 therapy was required in rabbits to achieve fungicidal activity in the cerebrum and
314 CSF.

315

316 **Pharmacokinetic-Pharmacodynamic Targets and Bridging Studies**

317 A human regimen of liposomal amphotericin B of 4 mg/kg/day produces an AUC_{0-24}
318 at steady state of ~ 190 mg.h/L. As can be seen in Figure 1 Panel F this is associated
319 with near-maximal antifungal efficacy in mice receiving daily liposomal amphotericin
320 B. A single dose of 20 mg/kg in mice (AUC_{0-24} 550-600 mg.h/L) also produced near
321 maximal antifungal activity. The bridging study in rabbits suggested that a single
322 dose of 5 mg/kg (AUC 833 mg.h/L) was insufficient to achieve fungicidal activity.
323 Rather, a total of three doses of 5 mg/kg/day (cumulative AUC 2499 mg.h/L) was
324 required to achieve fungicidal activity in the CSF. Thus, there was a degree of
325 discordance between the pharmacodynamic targets from mice and rabbits with the
326 latter requiring slightly more drug exposure to achieve the same effect.

327

328 **DISCUSSION**

329 Amphotericin B is the most potent agent for induction therapy against *Cryptococcus*
330 *neoformans*, and the combination with flucytosine results in the most rapid overall
331 decline in fungal burden (22). This study suggests that abbreviated regimens of
332 liposomal amphotericin B may be feasible. This is primarily a function of a
333 favourable pharmacokinetic profile with long terminal elimination phases in both the
334 plasma and brain ($t_{1/2}$ 133 hours).

335

336 The apparent discordance between plasma concentrations of liposomal amphotericin
337 B and its persistent anti-cryptococcal activity in the central nervous system (CNS) of
338 both mice and rabbits is of considerable interest, although the underlying mechanism
339 driving this phenomenon is not entirely clear. One possibility is that there are a
340 limited number of binding sites for amphotericin B in the central nervous system.
341 Once occupied, amphotericin B does not readily disengage from its binding sites
342 leading to a pharmacologically active depot of drug. A relatively short course of
343 liposomal amphotericin B (e.g. 1-3 doses) is all that is required to fully occupy these
344 binding sites and result in persistent antifungal activity. Further doses are simply
345 redundant and only serve to increase the probability of toxicity. The persistent
346 occupation of receptors results in a sustained antifungal response for many days even
347 after plasma concentrations have declined to undetectable levels.

348

349 Exactly how liposomal amphotericin B traffics into the various clinically relevant
350 effect sites is not clear. Drug penetrates into CNS sub-compartments that are
351 structurally normal and with histological evidence of inflammation (e.g. the
352 ependyma in Figure 5D). The immunohistochemistry studies suggest the transfer
353 from blood to the CNS occurs relatively quickly (i.e. in the first 24 hours), but they do
354 not enable estimates of the rate of transfer of drug. We did not observe high
355 concentrations of drug within cryptococcomas where the blood-brain-barrier is likely
356 significantly disrupted, even though amphotericin B was readily quantifiable in
357 homogenates of cerebrum of mice. This is probably because the amphotericin B
358 immunoassay is relatively insensitive. We did not see any evidence of drug being
359 carried into cryptococcomas by inflammatory cells (the dump truck phenomenon) as

360 is described for macrolides (23) although there was a very limited inflammatory
361 response in this model.
362
363 While the study provides the experimental foundation for the concept of using
364 abbreviated induction regimens of liposomal amphotericin B for cryptococcal
365 meningitis, there is some uncertainty about the best regimen(s) for humans. Taken in
366 isolation, the rabbit studies suggest that more than a single dose is required (with a
367 cumulative AUC >833 mg.h/L). The AUC associated with a dose of 5 mg/kg i.v. in a
368 rabbit is higher than that observed following 20 mg/kg i.v. to a mouse (833 versus 555
369 mg.h/L, respectively) for which prolonged antifungal activity in the cerebrum was
370 observed (Figure 1). Thus, the mouse may underestimate the total (cumulative) drug
371 exposure required for fungicidal activity in humans. Estimates of appropriate
372 regimens are further complicated by some uncertainty in the PK of higher doses of
373 liposomal amphotericin B in humans. We recently described much greater drug
374 exposures (C_{max} and AUC) after multiple doses in at least some children receiving
375 up to 10 mg/kg of LAmB (20) although we did not observe this phenomenon with
376 high-dose intermittent dosing in adults (21). Further detailed PK studies of higher
377 doses of LAmB are warranted.
378
379 The current study has several limitations and assumptions. Firstly, we did not
380 examine whether immunological effectors may have had an additional antifungal
381 effect to that of LAmB, and whether this may have contributed to persistent
382 antifungal activity observed with single doses. There was no evidence from the
383 histopathological studies of an inflammatory infiltrate in either mice or rabbits (the
384 latter is not shown). We extensively investigated this possibility in a recent study that

385 examined the effect of abbreviated regimens of DAmB for cryptococcal
386 meningoencephalitis, in which there was no evidence of immune-mediated antifungal
387 killing (13). Secondly, we made an explicit assumption that the trafficking (both the
388 rate and extent) of drug from the bloodstream to the site of infection is the equivalent
389 in mice, rabbits and humans. Such an assumption is central to PK-PD bridging
390 studies for all drug-pathogen combinations. In the majority of cases, this assumption
391 is reasonable, but there are isolated examples where it is not (24). Thirdly, there
392 remains a degree of uncertainty regarding the lowest dose and shortest possible course
393 of LAmB that is likely to be effective for patients with cryptococcal
394 meningoencephalitis. We did not design this study to specifically address this
395 question, which would have required many more animals. Finally, we did not
396 examine optimal combinations of antifungal agents when one or both agents is
397 administered as a short course.

398

399 Given the overwhelming cost and feasibility advantages of abbreviated induction
400 therapy based on one or few doses of LAmB, clinical trials are now required to
401 further test these ideas. A two-stage adaptive open-label phase II/III randomised non-
402 inferiority trial comparing alternative short course LAmB regimens is underway and
403 will report in 2017 (trial registration number: ISRCTN10248064). These clinical trials
404 will provide information for new therapeutic options for this neglected infection.

405

406 **Acknowledgements:**

407 The authors acknowledge the helpful contributions of Andrew Sharp and Joanne
408 Goodwin.

409

410

411

412

413 Table 1. The parameters from the population pharmacokinetic-pharmacodynamic

414 model from mice, along with the estimates for the mean, median and standard

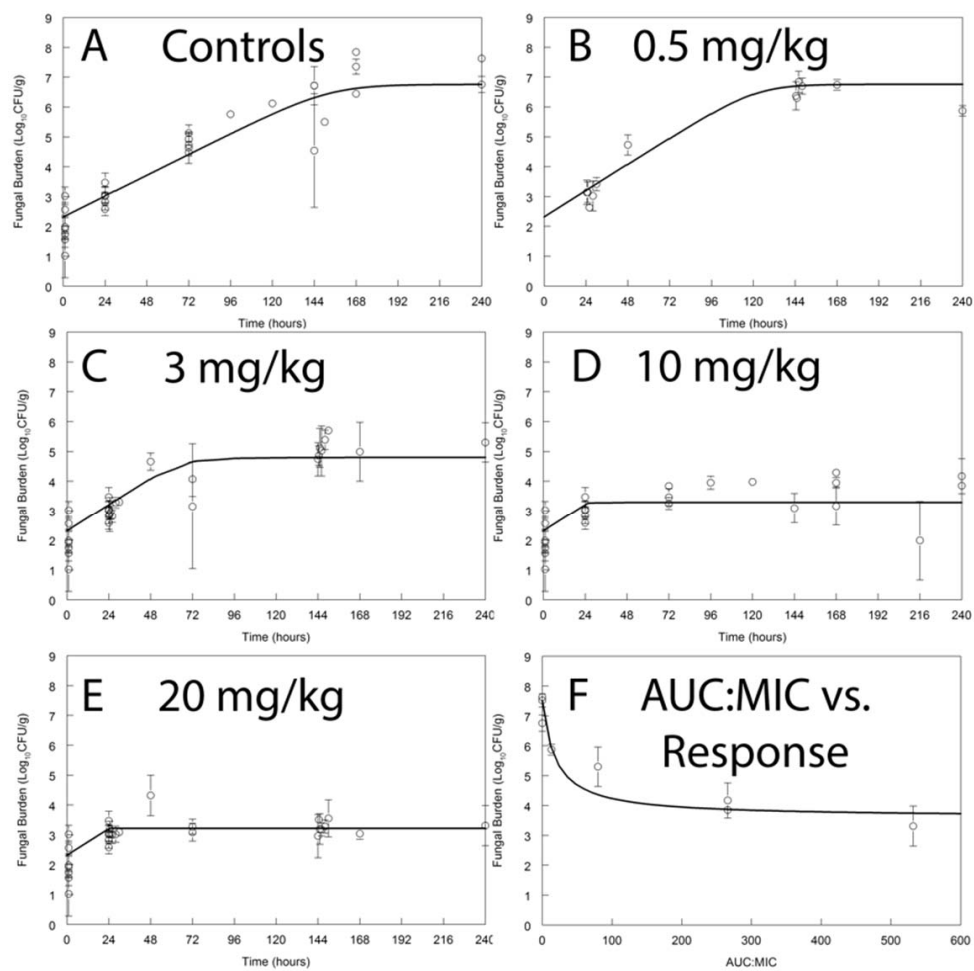
415 deviation. Parameter values are as described in the text.

416

Parameter (Units)	Mean	Median	Standard Deviation
SCL (liters/h)	0.00082	0.00094	0.00018
Volume (liters)	0.003	0.0027	0.0019
Kcp (h ⁻¹)	11.99	10.52	9.94
Kpc (h ⁻¹)	15.70	23.33	11.41
Kcb (h ⁻¹)	0.16	0.22	0.013
Kbc (h ⁻¹)	0.034	0.01	0.038
Kgmax (log ₁₀ CFU/g/h)	0.096	0.084	0.033
Hg	7.96	7.72	6.00
C _{50g} (mg/L)	0.088	0.056	0.100
POPMAX (CFU/g)	23785100	57435030	249007
Vm (liters)	0.72	0.94	0.37
Initial Condition (CFU/g)	186	207	133.97

417

418



419

420 Figure 1. Pharmacodynamics of liposomal amphotericin B (LAmB) in cohorts of

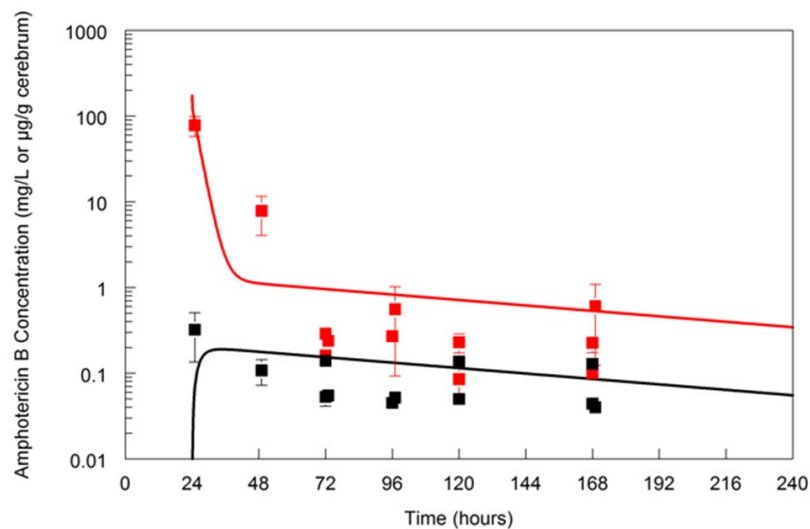
421 mice receiving 0.5 (Panel B), 3 (Panel C), 10 (Panel D) and 20 mg/kg/day i.v. (Panel

422 E). The area under the concentration time curve (AUC:MIC) at steady state versus

423 the observed fungal density at the end of the experiment (time = 240 hours) is shown

424 in Panel F. All data are mean \pm standard deviation from groups of three mice.

425



426

427

428 Figure 2. The pharmacokinetics of liposomal amphotericin B (LAmB) in murine

429 plasma (red line and red data points) and cerebrum (black line and black data points)

430 in cohorts of mice infected with *Cryptococcus neoformans* receiving LAmB 20 mg/kg431 once i.v. (24 hours post inoculation). All data are mean \pm standard deviation from

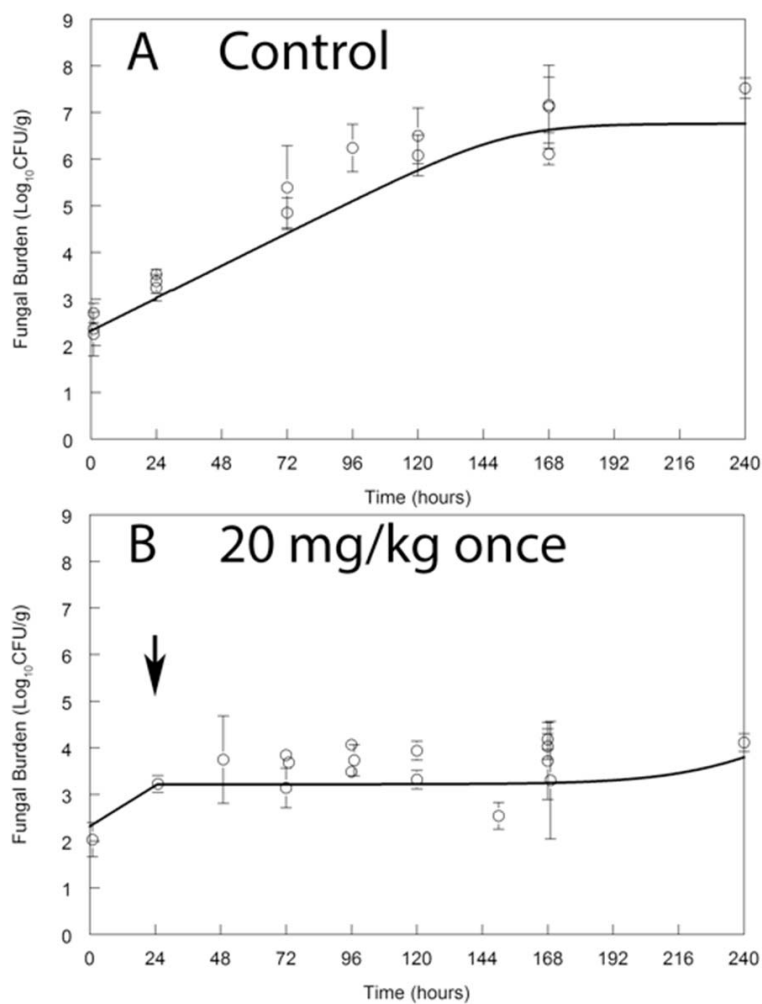
432 groups of three mice. The terminal half-life in the plasma and cerebrum is circa 133

433 hours.

434

435

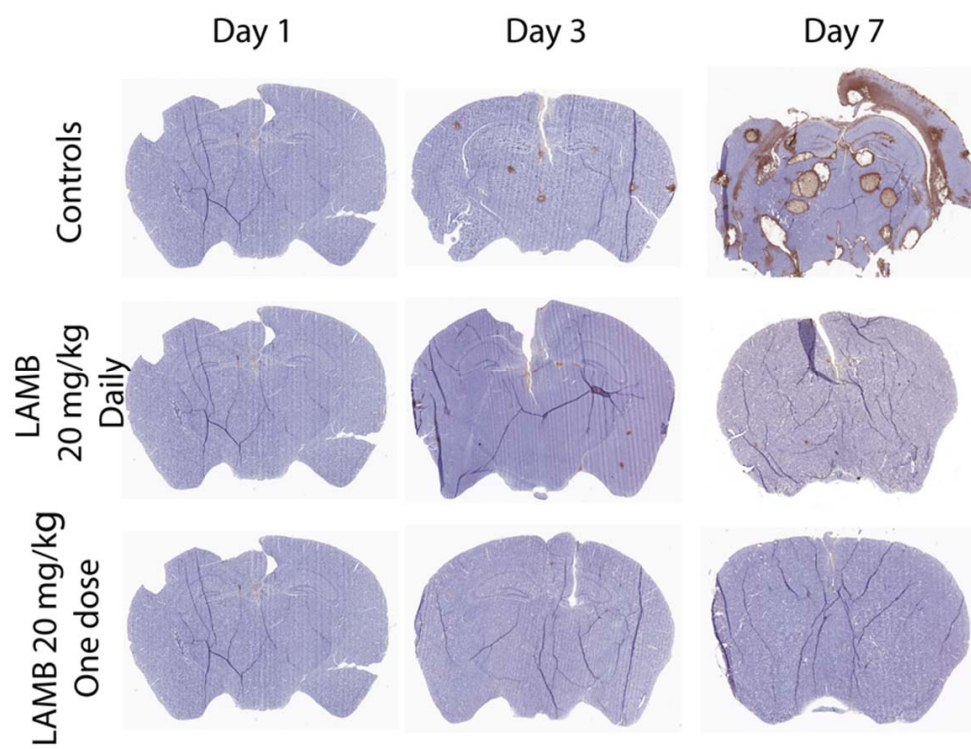
436



437

438

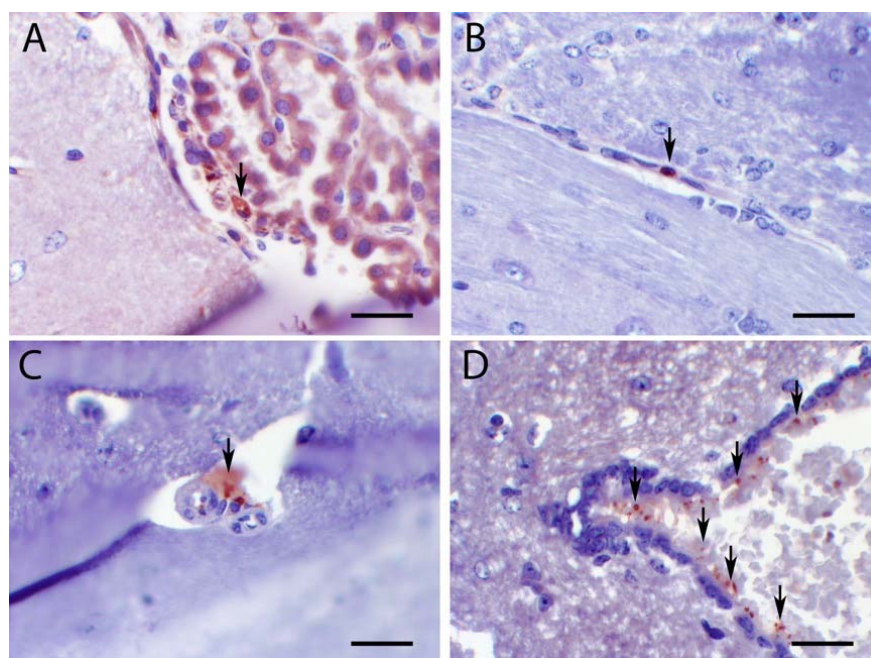
439 Figure 3. The pharmacodynamics of vehicle control (Panel A) and liposomal
440 amphotericin B (Panel B) following the administration of a single dose of 20 mg/kg
441 i.v. to mice with cryptococcal meningoencephalitis. Data are the mean \pm standard
442 deviation from groups of three mice. The solid line is the fit of the mathematical PK-
443 PD model (parameters summarised in Table 1). The black arrow denotes the time of
444 drug administration relative to inoculation (which occurred at time=0).



445

446 Figure 4. Representative cross sections of brains from mice receiving vehicle control,
447 LAMB 20 mg/kg/day i.v. and LAMB 20 mg/kg once i.v. Each section has been
448 stained with an anti-cryptococcal antibody and then counter stained with hematoxylin.
449 Treatment was initiated at the end of Day 1 (i.e. 24 hours post inoculation). There are
450 multiple cryptococcomas at the end of Day 7 in untreated controls. In contrast there
451 are relatively few and exceedingly small lesions in both treatment groups.

452



453

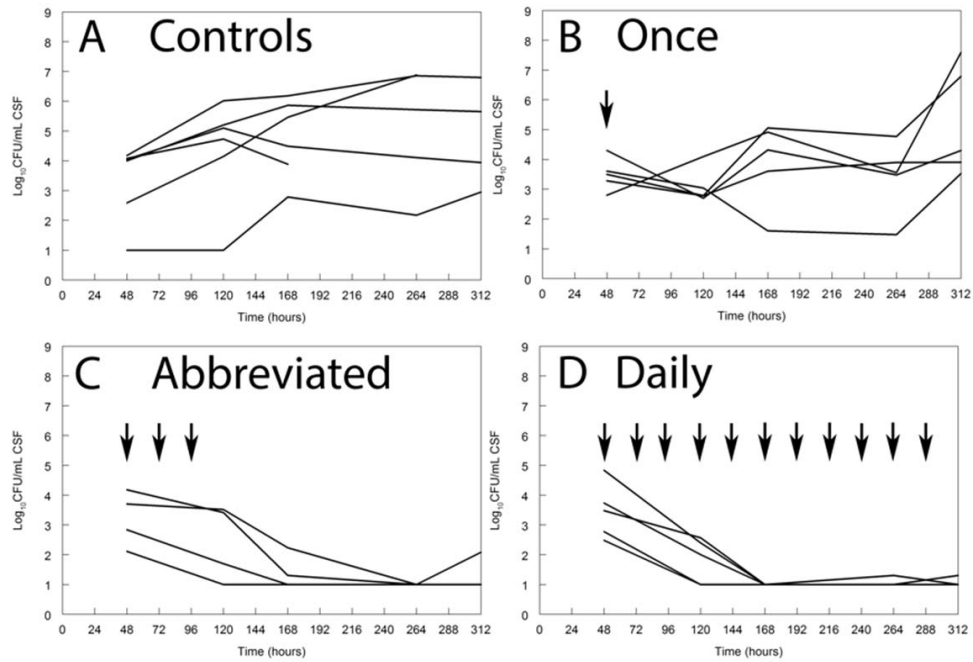
454

455 Figure 5. Distribution of liposomal amphotericin B (LAmB) in the central nervous
456 system. All mice received LAmB 20 mg/kg i.v.. In each panel the black arrows show
457 areas of staining of amphotericin B. Panel A, LAmB staining in the choroid plexus
458 (extracellular and within a macrophage); Panel B, positive LAmB staining within a
459 mononuclear cell in a thin-walled cerebral capillary; Panel C, positive staining in a
460 perivascular location, adjacent to a thick-walled small arteriole; Panel D, LAmB
461 staining in CSF associated with apical surface of in ependymal cells, cerebral
462 aqueduct. Scale bars 5 μ m in Panels A, B and D. Scale bar 25 μ m in Panel C.

463

464

465



466

467 Figure 6. The time course of fungal density in the CSF of rabbits following various
468 regimens of liposomal amphotericin B. Each line represents the data from a single
469 rabbit. Each animal received 5 mg/kg every 24 hours. The time course of fungal
470 density in the CSF in rabbits receiving a single dose of drug (Panel B) is comparable
471 to controls shown in Panel A. An abbreviated regimen of 5 mg/kg/day for 3 doses
472 results in prompt fungicidal activity that is comparable to daily therapy with the same
473 dose.

474

475

476

477

478

479 REFERENCES

- 480 1. **Jarvis JN, Bicanic T, Loyse A, Namarika D, Jackson A, Nussbaum JC,**
481 **Longley N, Muzoora C, Phulusa J, Taseera K, Kanyembe C, Wilson D,**
482 **Hosseini pour MC, Brouwer AE, Limmathurotsakul D, White N, van der**
483 **Horst C, Wood R, Meintjes G, Bradley J, Jaffar S, Harrison T.** 2014.
484 Determinants of mortality in a combined cohort of 501 patients with HIV-
485 associated Cryptococcal meningitis: implications for improving outcomes.
486 *Clin Infect Dis* **58**:736-745.
- 487 2. **Bicanic T, Muzoora C, Brouwer AE, Meintjes G, Longley N, Taseera K,**
488 **Rebe K, Loyse A, Jarvis J, Bekker LG, Wood R, Limmathurotsakul D,**
489 **Chierakul W, Stepniewska K, White NJ, Jaffar S, Harrison TS.** 2009.
490 Independent association between rate of clearance of infection and clinical
491 outcome of HIV-associated cryptococcal meningitis: analysis of a combined
492 cohort of 262 patients. *Clin Infect Dis* **49**:702-709.
- 493 3. **Al-Nakeeb Z, Petraitis V, Goodwin J, Petraitiene R, Walsh TJ, Hope**
494 **WW.** 2015. Pharmacodynamics of amphotericin B deoxycholate,
495 amphotericin B lipid complex, and liposomal amphotericin B against
496 *Aspergillus fumigatus*. *Antimicrob Agents Chemother* **59**:2735-2745.
- 497 4. **Lestner JM, Howard SJ, Goodwin J, Gregson L, Majithiya J, Walsh TJ,**
498 **Jensen GM, Hope WW.** 2010. Pharmacokinetics and pharmacodynamics of
499 amphotericin B deoxycholate, liposomal amphotericin B, and amphotericin B
500 lipid complex in an in vitro model of invasive pulmonary aspergillosis.
501 *Antimicrob Agents Chemother* **54**:3432-3441.
- 502 5. **Bicanic T, Bottomley C, Loyse A, Brouwer AE, Muzoora C, Taseera K,**
503 **Jackson A, Phulusa J, Hosseini pour MC, van der Horst C,**

- 504 **Limmathurotsakul D, White NJ, Wilson D, Wood R, Meintjes G,**
505 **Harrison TS, Jarvis JN.** 2015. Toxicity of Amphotericin B Deoxycholate-
506 Based Induction Therapy in Patients with HIV-Associated Cryptococcal
507 Meningitis. *Antimicrob Agents Chemother* **59**:7224-7231.
- 508 6. **Wingard JR, Kubilis P, Lee L, Yee G, White M, Walshe L, Bowden R,**
509 **Anaissie E, Hiemenz J, Lister J.** 1999. Clinical significance of
510 nephrotoxicity in patients treated with amphotericin B for suspected or proven
511 aspergillosis. *Clin Infect Dis* **29**:1402-1407.
- 512 7. **Longley N, Muzoora C, Taseera K, Mwesigye J, Rwebembera J, Chakera**
513 **A, Wall E, Andia I, Jaffar S, Harrison TS.** 2008. Dose response effect of
514 high-dose fluconazole for HIV-associated cryptococcal meningitis in
515 southwestern Uganda. *Clin Infect Dis* **47**:1556-1561.
- 516 8. **Nussbaum JC, Jackson A, Namarika D, Phulusa J, Kenala J, Kanyemba**
517 **C, Jarvis JN, Jaffar S, Hosseinipour MC, Kamwendo D, van der Horst**
518 **CM, Harrison TS.** 2010. Combination flucytosine and high-dose fluconazole
519 compared with fluconazole monotherapy for the treatment of cryptococcal
520 meningitis: a randomized trial in Malawi. *Clin Infect Dis* **50**:338-344.
- 521 9. **Hamill RJ, Sobel JD, El-Sadr W, Johnson PC, Graybill JR, Javaly K,**
522 **Barker DE.** 2010. Comparison of 2 doses of liposomal amphotericin B and
523 conventional amphotericin B deoxycholate for treatment of AIDS-associated
524 acute cryptococcal meningitis: a randomized, double-blind clinical trial of
525 efficacy and safety. *Clin Infect Dis* **51**:225-232.
- 526 10. **O'Connor L, Livermore J, Sharp AD, Goodwin J, Gregson L, Howard**
527 **SJ, Felton TW, Schwartz JA, Neely MN, Harrison TS, Perfect JR, Hope**
528 **WW.** 2013. Pharmacodynamics of liposomal amphotericin B and flucytosine

- 529 for cryptococcal meningoencephalitis: safe and effective regimens for
530 immunocompromised patients. *J Infect Dis* **208**:351-361.
- 531 11. **Perfect JR, Dismukes WE, Dromer F, Goldman DL, Graybill JR, Hamill**
532 **RJ, Harrison TS, Larsen RA, Lortholary O, Nguyen MH, Pappas PG,**
533 **Powderly WG, Singh N, Sobel JD, Sorrell TC.** 2010. Clinical practice
534 guidelines for the management of cryptococcal disease: 2010 update by the
535 infectious diseases society of america. *Clin Infect Dis* **50**:291-322.
- 536 12. **Sloan DJ, Dedicoat MJ, Lalloo DG.** 2009. Treatment of cryptococcal
537 meningitis in resource limited settings. *Curr Opin Infect Dis* **22**:455-463.
- 538 13. **Livermore J, Howard SJ, Sharp AD, Goodwin J, Gregson L, Felton T,**
539 **Schwartz JA, Walker C, Moser B, Muller W, Harrison TS, Perfect JR,**
540 **Hope WW.** 2014. Efficacy of an abbreviated induction regimen of
541 amphotericin B deoxycholate for cryptococcal meningoencephalitis: 3 days of
542 therapy is equivalent to 14 days. *MBio* **5**:e00725-00713.
- 543 14. **Muzoora CK, Kabanda T, Ortu G, Ssentamu J, Hearn P, Mwesigye J,**
544 **Longley N, Jarvis JN, Jaffar S, Harrison TS.** 2012. Short course
545 amphotericin B with high dose fluconazole for HIV-associated cryptococcal
546 meningitis. *J Infect* **64**:76-81.
- 547 15. **Perfect JR, Lang SD, Durack DT.** 1980. Chronic cryptococcal meningitis: a
548 new experimental model in rabbits. *Am J Pathol* **101**:177-194.
- 549 16. **Sudan A, Livermore J, Howard SJ, Al-Nakeeb Z, Sharp A, Goodwin J,**
550 **Gregson L, Warn PA, Felton TW, Perfect JR, Harrison TS, Hope WW.**
551 2013. Pharmacokinetics and pharmacodynamics of fluconazole for
552 cryptococcal meningoencephalitis: implications for antifungal therapy and in
553 vitro susceptibility breakpoints. *Antimicrob Agents Chemother* **57**:2793-2800.

- 554 17. **Clemons KV, Schwartz JA, Stevens DA.** 2012. Experimental central
555 nervous system aspergillosis therapy: efficacy, drug levels and localization,
556 immunohistopathology, and toxicity. *Antimicrob Agents Chemother* **56**:4439-
557 4449.
- 558 18. **Smith PJ, Olson JA, Constable D, Schwartz J, Proffitt RT, Adler-Moore**
559 **JP.** 2007. Effects of dosing regimen on accumulation, retention and
560 prophylactic efficacy of liposomal amphotericin B. *J Antimicrob Chemother*
561 **59**:941-951.
- 562 19. **Neely MN, van Guilder MG, Yamada WM, Schumitzky A, Jelliffe RW.**
563 2012. Accurate detection of outliers and subpopulations with Pmetrics, a
564 nonparametric and parametric pharmacometric modeling and simulation
565 package for R. *Ther Drug Monit* **34**:467-476.
- 566 20. **Lestner JM, Groll AH, Aljayoussi G, Seibel NL, Shad A, Gonzalez C,**
567 **Wood LV, Jarosinski PF, Walsh TJ, Hope WW.** 2016. Population
568 Pharmacokinetics of Liposomal Amphotericin B in Immunocompromised
569 Children. *Antimicrob Agents Chemother* **60**:7340-7346.
- 570 21. **Hope WW, Goodwin J, Felton TW, Ellis M, Stevens DA.** 2012. Population
571 pharmacokinetics of conventional and intermittent dosing of liposomal
572 amphotericin B in adults: a first critical step for rational design of innovative
573 regimens. *Antimicrob Agents Chemother* **56**:5303-5308.
- 574 22. **Day JN, Chau TT, Lalloo DG.** 2013. Combination antifungal therapy for
575 cryptococcal meningitis. *N Engl J Med* **368**:2522-2523.
- 576 23. **Drusano GL.** 2005. Infection site concentrations: their therapeutic importance
577 and the macrolide and macrolide-like class of antibiotics. *Pharmacotherapy*
578 **25**:150S-158S.

- 579 24. **Warner DF, Mizrahi V.** 2014. Shortening treatment for tuberculosis--to
580 basics. *N Engl J Med* **371**:1642-1643.
581

